CHAPTER 3

HYDROMAGNETIC LUBRICATION OF POROUS BEARINGS

The studies of the effect of a magnetic field on the flow of a conducting fluid show that hydromagnetic bearings have several advantages. Such bearings not only carry more load than ordinary bearings, but they can carry loads even when the equivalent conventional bearings have no load capacity. According to Kuzma [44] friction can be reduced to zero by applying proper magnetic fields and the transient loads have less effect on hydromagnetic bearings than on ordinary bearings.

Sintered metal self-lubricating bearings are advantageous for many applications owing to various reasons discussed earlier. Although the bearing characteristics suffer because of porosity, the numerous design and maintenance advantages overcome these. Efforts were made to improve bearing characteristics by the application of electromagnetic fields [5, 27].

In the following sections we study the effect of a transverse magnetic field on the lubrication of two-layered porous rectangular plates and an inclined slider. We shall see that the effect of porosity in decreasing the load capacity can be countered by the application of a magnetic field. But the increase in load capacity comes at the expense of increased friction.

3.1 HYDROMAGNETIC SQUEEZE FILM BETWEEN TWO-LAYERED POROUS PARALLEL RECTANGULAR PLATES

The squeeze film between two parallel plates, one with a porous facing, was investigated by many persons [5, 10, 17, 18]. In these investigations the porous facing had the same permeability throughout.

Cusano [6, 45] showed that the seepage through the boundary of the porous bearing, which causes the decrease in load capacity, might be decreased by the use of multi-layered porous housing of different permeabilities, thus improving the bearing performance. He showed that in a narrow bearing and an infinitely long bearing, a low permeability inner layer increased the load capacity and decreased the coefficient of friction.

In this section we study the squeeze film behaviour between two parallel rectangular plates, when the upper plate has a porous housing of two layers with different permeabilities, in the presence of a uniform transverse magnetic field.

3.1.1 Mathematical formulation

Consider a fluid film of thickness h between two parallel rectangular plates where the lower plate remains fixed and the upper plate is assumed to move normal to itself. The upper plate has a two-layer porous housing of thickness $H = H_1 + H_2$ with permeabilities k_1, k_2 of the lower and upper layers respectively. A uniform magnetic field B_0 is applied perpendicular to the plates as in Fig. 7. Flows in the porous regions follow the modified Darcy's law [11]. In the film region the equations of hydromagnetic lubrication theory hold. Following the assumptions of porous metal hydromagnetic lubrication of section 1.2, the basic equations governing the hydromagnetic flow of the lubricant in different regions are obtained as :

Film region :

$$\frac{\partial^2 u}{\partial y^2} - \frac{M^2}{h_0^2} u = \frac{1}{\mu} \frac{\partial p}{\partial x} \tag{1}$$

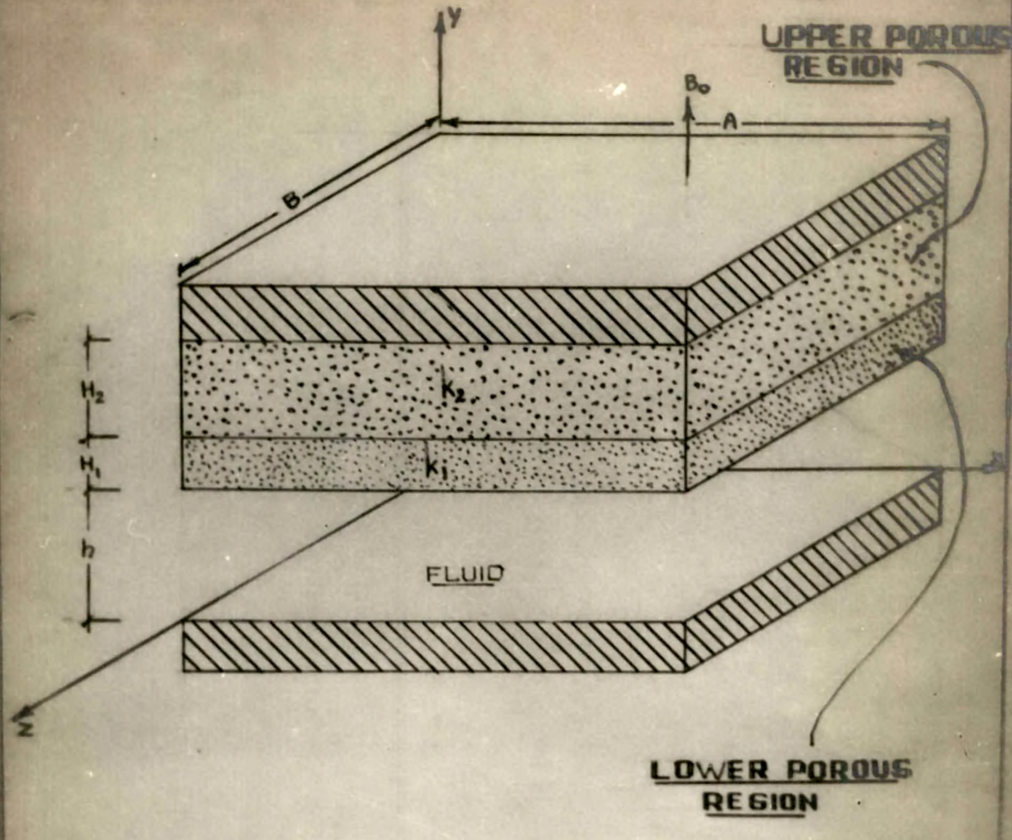

FIG. 7. SQUEEZE FILM BETWEEN TWO-LAYERED POROUS RECTANGULAR PARALLEL PLATES.

$$\frac{\partial p}{\partial y} = 0 \tag{2}$$

$$\frac{\partial^2 w}{\partial y^2} - \frac{M^2}{h_0^2} w = \frac{1}{\mu} \frac{\partial p}{\partial z} \tag{3}$$

$$\frac{\partial u}{\partial x} + \frac{\partial v}{\partial y} + \frac{\partial w}{\partial z} = 0 \tag{4}$$

Lower porous region :

$$V_x = - \frac{k_1}{\mu} \frac{\partial P_1}{\partial x} \frac{1}{c_1^2} \tag{5}$$

$$V_y = - \frac{k_1}{\mu} \frac{\partial P_1}{\partial y} \tag{6}$$

$$V_z = - \frac{K_1}{\mu} \frac{\partial P_1}{\partial z} \frac{1}{c_1^2} \tag{7}$$

$$\frac{\partial V_x}{\partial x} + \frac{\partial V_y}{dy} + \frac{\partial V_z}{dz} = 0 \tag{8}$$

Upper porous region :

$$V_x^* = - \frac{k_2}{\mu} \frac{\partial P_2}{\partial x} \frac{1}{c_2^2} \tag{9}$$

$$V_y^* = -\frac{k_2}{\mu} \frac{\partial P_2}{\partial y} \tag{10}$$

$$V_z^* = -\frac{k_2}{\mu} \frac{\partial P_2}{\partial z} \frac{1}{c_2^2} \tag{11}$$

$$\frac{\partial V_x^*}{\partial x} + \frac{\partial V_y^*}{\partial y} + \frac{\partial V_z^*}{\partial z} = 0 \tag{12}$$

where

$$M = B_0 h_0 \sqrt{\sigma / \mu} \quad , \quad c_1 = \left(1 + \frac{k_1}{m_1} \frac{M^2}{h_0^2}\right)^{1/2}$$

and

$$c_2 = \left(1 + \frac{k_2}{m_2} \frac{M^2}{h_0^2}\right)^{1/2}. \tag{13}$$

From equations (5) - (12) it follows that the fluid pressures P_1 and P_2 in the porous regions satisfy the equations

$$\frac{\partial^2 P_1}{\partial x^2} + \frac{\partial^2 P_1}{\partial z^2} + c_1^2 \frac{\partial^2 P_1}{\partial y^2} = 0 \tag{14}$$

$$\frac{\partial^2 P_2}{\partial x^2} + \frac{\partial^2 P_2}{\partial z^2} + c_2^2 \frac{\partial^2 P_2}{\partial y^2} = 0 \tag{15}$$

The solutions of equations (1) and (3) subject to the no-slip conditions on both the surfaces are

$$u = \frac{h_0^2}{\mu M^2} \frac{\partial p}{\partial x} \left[\left(\cosh \frac{My}{h_0} - 1\right) - \left(\cosh \frac{Mh}{h_0} - 1\right) \frac{\sinh \frac{My}{h_0}}{\sinh \frac{Mh}{h_0}} \right] \tag{16}$$

and

$$w = \frac{h_0^2}{\mu M^2} \frac{\partial p}{\partial z} \left[\left(\cosh \frac{My}{h_0} - 1\right) - \left(\cosh \frac{Mh}{h_0} - 1\right) \frac{\sinh \frac{My}{h_0}}{\sinh \frac{Mh}{h_0}} \right] \tag{17}$$

Substituting equations (16) and (17) into equation (..4) and integrating across the film thickness h, keeping in view that the lower plate is non-porous and fixed, we have

$$v_h = \frac{h_0^3}{\mu M^3} \left(\frac{\partial^2 p}{\partial x^2} + \frac{\partial^2 p}{\partial z^2} \right) \left[\frac{Mh}{h_0} - 2 \tanh \frac{Mh}{2h_0} \right] . \tag{18}$$

Since the velocity component in the y-direction is continuous at the plate-film interface ,

$$v_h - \frac{dh}{dt} = (V_y)_{y=h} = - \frac{k_1}{\mu} \left(\frac{\partial P_1}{\partial y} \right)_{y=h} \tag{19}$$

From equations (18) and (19), the fluid pressure in the film region is found to satisfy the equation

$$\frac{\partial^2 p}{\partial x^2} + \frac{\partial^2 p}{\partial z^2} = \frac{\frac{dh}{dt} - \frac{k_1}{\mu} \left(\frac{\partial P_1}{\partial y} \right)_{y=h}}{\frac{h_0^3}{\mu M^3} \left(\frac{Mh}{h_0} - 2 \tanh \frac{Mh}{2h_0} \right)} . \tag{20}$$

The associated boundary conditions with equations (14),(15) and (20) are

$$p(x,\ 0) = 0 \tag{21}$$

$$p(x,\ B) = 0 \tag{22}$$

$$p(0,\ z) = 0 \tag{23}$$

$$p(A, z) = 0 \tag{24}$$

$$P_1(x, y, 0) = 0 \tag{25}$$

$$P_1(x, y, B) = 0 \tag{26}$$

$$P_1(0, y, z) = 0 \tag{27}$$

$$P_1(A, y, z) = 0 \tag{28}$$

$$P_2(x, y, 0) = 0 \tag{29}$$

$$P_2(x, y, B) = 0 \tag{30}$$

$$P_2(0, y, z) = 0 \tag{31}$$

$$P_2(A, y, z) = 0. \tag{32}$$

Since the normal velocity components and the pressures must be continuous at the interfaces

$$\left(\frac{\partial P_2}{\partial y} \right)_{y = h+H_1+H_2} = 0 \tag{33}$$

$$k_1 \left(\frac{\partial P_1}{\partial y} \right)_{y = h+H_1} = k_2 \left(\frac{\partial P_2}{\partial y} \right)_{y = h+H_1} \tag{34}$$

$$P_1(x,\ h + H_1\ ,\ z) = P_2(x,\ h + H_1,\ z) \tag{35}$$

$$p(x,\ z) \quad = P_1(x,\ h,\ z). \tag{36}$$

The problem is a coupled one in view of equation (20) and the coupled boundary conditions (34) - (36).

3.1.2 <u>Solutions</u>

Solutions of equations (14) and (15) with the corresponding uncoupled boundary conditions are obtained as

$$P_1(x,\ y,\ z) = \sum_{m=1}^{\infty} \sum_{n=1}^{\infty} A'_{mn} \sin \alpha_m x \sin \beta_n z . e^{r_{mn} y/c_1}$$

$$.(1 + B'_{mn} \quad e^{-2r_{mn}\ y/c_1}) \tag{37}$$

and

$$P_2(x,\ y,\ z) = \sum_{m=1}^{\infty} \sum_{n=1}^{\infty} A_{mn} \sin \alpha_m x \sin \beta_n z . e^{r_{mn} y/c_2}$$

$$.(1 + e^{2r_{mn}\ (h + H_1 + H_2 - y)/c_2}) \tag{38}$$

where

$$\alpha_m = \frac{m\pi}{A}\ ,\ \beta_n = \frac{n\pi}{B}\ ,\ d = \frac{A}{B} \text{ and } r_{mn} = \frac{\pi}{A}\ (m^2+d^2n^2)^{1/2}. \tag{39}$$

According to equations (36) and (37)

$$p(x,\ z) = \sum_{m=1}^{\infty} \sum_{n=1}^{\infty} B_{mn} \sin \alpha_m x \sin \beta_n z \qquad (40)$$

with

$$B_{mn} = A'_{mn} \ e^{r_{mn} h/c_1} (1 + B'_{mn} \ e^{-2 r_{mn} \ h/c_1}). \qquad (41)$$

The solution of p as given by (40) satisfies the conditions (21) - (24).

From condition (35) and equations (37)-(38)

$$A_{mn} \ e^{r_{mn}(h + H_1)/c_2} (1 + e^{2 r_{mn} \ H_2/c_2})$$

$$= A'_{mn} \ e^{r_{mn} \ (h + H_1)/c_1} (1 + B'_{mn} \ e^{-2 r_{mn} (h+H_1)/c_1}) \qquad (42)$$

Use of equation (42) in equations (37) and (41) respectively gives

$$P_1(x, y, z) = \sum_{m=1}^{\infty} \sum_{n=1}^{\infty} A_{mn} \, G_{mn} \, e^{r_{mn}(y-h)/c_1}$$

$$\cdot \frac{1 + B'_{mn} \, e^{-2r_{mn} \, y/c_1}}{1 + B'_{mn} \, e^{-2r_{mn}(h+H_1)/c_1}} \sin \alpha_m x \sin \beta_n z \qquad (43)$$

and

$$B_{mn} = A_{mn} \, G_{mn} \frac{1 + B'_{mn} \, e^{-2r_{mn} \, h/c_1}}{1 + B'_{mn} \, e^{-2r_{mn}(h+H_1)/c_1}} \qquad (44)$$

where

$$G_{mn} = e^{r_{mn}(h+H_1)\left(\frac{1}{c_2} - \frac{1}{c_1}\right)} \left(1 + e^{2r_{mn}H_2/c_2}\right) e^{r_{mn}h/c_1} \qquad (45)$$

Using equations (37) - (38) in (34)

$$B'_{mn} = \frac{1 - F_{mn}}{1 + F_{mn}} \, e^{2r_{mn}(h + H_1)/c_1} \qquad (46)$$

where

$$F_{mn} = \frac{k_2 c_1}{k_1 c_2} \; \frac{1 - e^{2 r_{mn} H_2/c_2}}{1 + e^{2 r_{mn} H_2/c_2}} \tag{47}$$

Substitution of equations (44) and (46) in equation (40) yields

$$p(x,z) = \sum_{m=1}^{\infty} \sum_{n=1}^{\infty} A_{mn} \, G_{mn} \, \frac{1 + F_{mn} + (1 - F_{mn}) e^{2 r_{mn} H_1/c_1}}{2}$$

$$\cdot \sin \alpha_m x \sin \beta_n z. \tag{48}$$

Substitution of equation (46) in equation (43) gives

$$P_1(x,y,z) = \sum_{m=1}^{\infty} \sum_{n=1}^{\infty} A_{mn} \, G_{mn} \, e^{r_{mn} (y-h)/c_1}$$

$$\cdot \frac{1+F_{mn}+(1-F_{mn}) e^{2 r_{mn}(h+H_1-y)/c_1}}{2} \sin \alpha_m x \sin \beta_n z. \tag{49}$$

Using equations (48) and (49) in equation (20) and simplifying,

$$\frac{dh}{dt} = \sum_{m=1}^{\infty} \sum_{n=1}^{\infty} A_{mn} \, G_{mn} \, C_{mn} \, \frac{1 + F_{mn} + (1 - F_{mn}) e^{2 r_{mn} H_1 / c_1}}{2}$$

$$\cdot \sin \alpha_m x \sin \beta_n z \qquad (50)$$

where

$$C_{mn} = \frac{k_1}{\mu} \frac{r_{mn}}{c_1} \frac{1 + F_{mn} - (1 - F_{mn}) e^{2 r_{mn} H_1 / c_1}}{1 + F_{mn} + (1 - F_{mn}) e^{2 r_{mn} H_1 / c_1}}$$

$$- \frac{h_0^3}{\mu M^3} r_{mn}^2 \left(\frac{Mh}{h_0} - 2 \tanh \frac{Mh}{2h_0} \right). \qquad (51)$$

The constants A_{mn} are obtained by using the orthogonality of the eigen functions $\sin \alpha_m x$, $\sin \beta_n z$ in equation (50) as

$$A_{mn} = \begin{cases} \dfrac{16 \frac{dh}{dt}}{mn\pi^2 \, G_{mn} C_{mn}} \cdot \dfrac{2}{1+F_{mn}+(1-F_{mn}) e^{2 r_{mn} H_1 / c_1}} & \text{if } m,n \text{ are odd} \\ 0 , & \text{otherwise} \end{cases} \qquad (52)$$

Substituting from (52) in equation (48), the pressure distribution in the film region is obtained as

$$p(x,\ z) = \sum_{m,n\ odd}^{\infty} \sum^{\infty} \frac{16 \frac{dh}{dt}}{mn\ \pi^2\ C_{mn}} \sin \alpha_m x \sin \beta_n z, \tag{53}$$

where C_{mn} is given by (51).

In dimensionless form it becomes

$$\bar{p}(x,\ z) = - \frac{dt}{dh} \frac{h^3 p}{\mu A^2}$$

$$= \frac{16}{\pi^3} \sum_{m,n\ odd}^{\infty} \sum^{\infty} \frac{\sin \alpha_m x \sin \beta_n z}{mn(m^2 + d^2 n^2)^{1/2}}$$

$$\cdot \left[\frac{\pi}{M^3 \bar{h}^3} (m^2 + d^2 n^2)^{1/2} (M\bar{h} - 2 \tanh \frac{M\bar{h}}{2}) + \frac{\Psi_1}{c_1 \bar{h}^3} D_{mn} \right]^{-1} \tag{54}$$

where

$$\bar{h} = \frac{h}{h_0}, \quad \Psi_1 = \frac{k_1 H}{h_0^3}, \quad \bar{H} = \frac{H}{A} \tag{55}$$

and

$$D_{mn} = \frac{(1 - F_{mn}) e^{2r_{mn} H_1/c_1} - (1 + F_{mn})}{\bar{H} \left[(1 - F_{mn}) e^{2r_{mn} H_1/c_1} + (1 + F_{mn}) \right]} . \quad (56)$$

The load capacity is obtained by integrating the pressure over the area of the plate :

$$W = \int_0^B \int_0^A p(x,z) \, dxdz. \quad (57)$$

In dimensionless form it is obtained as

$$\bar{W} = - \frac{dt}{dh} \frac{h^3 W}{\mu A^3 B} = \frac{64}{\pi^5} \sum_{m,n}^{\infty} \sum_{odd}^{\infty} \frac{1}{m^2 n^2 (m^2 + d^2 n^2)^{1/2}}$$

$$\cdot \left[\frac{\pi}{M^3 \bar{h}^3} (m^2 + d^2 n^2)^{1/2} (M\bar{h} - 2 \tanh \frac{M\bar{h}}{2}) + \frac{\Psi_1}{c_1 \bar{h}^3} D_{mn} \right]^{-1} \quad (58)$$

From equation (58), the time of approach as the function of height h, for a given load W, is given by

$$\int_{t_o}^{t_1} dt = -64 \frac{\mu A^3 B}{\pi^6 h_0^2 W} \sum_{m,n}^{\infty} \sum_{odd}^{\infty} \left[\frac{M^3}{m^2 n^2 (m^2 + d^2 n^2)} \right.$$

$$\left. \cdot \int_1^{\bar{h}} \frac{d\bar{h}}{M\bar{h} - 2\tanh \frac{M\bar{h}}{2} + E_{mn}} \right] \qquad (59)$$

where

$$E_{mn} = \frac{M^3 \psi_1 D_{mn}}{c_1 \pi (m^2 + d^2 n^2)^{1/2}} \qquad (60)$$

As the asymptotic solutions of equation (59) are of little practical interest for small values of M, the integral on the right of equation (59) is evaluated for large Hartmann numbers. Assuming that the initial film thickness is h_0 at $t_o = 0$, the time of approach in dimensionless form is obtained as

$$\Delta T = \frac{h_0^2 W}{\mu A^3 B} \Delta t$$

$$= -\frac{64}{\pi^6} \sum_{m,n}^{\infty} \sum_{odd}^{\infty} \frac{M^2 \ln \left(\frac{E_{mn} - 2 + M\bar{h}}{E_{mn} - 2 + M} \right)}{m^2 n^2 (m^2 + d^2 n^2)} \cdot \qquad (61)$$

In particular, if $H_2 = 0$, $H_1 = H$, $c_1 = c$, $k_1 = k$ are taken, the results when the upper plate has the same permeability confirm those of Sinha and Gupta [5].

3.1.3 Results and discussion

Equation (58) gives the load carrying capacity of the bearing and equation (61) expresses the time of approach as a function of film thickness. The main parameters affecting bearing characteristics are M, $\frac{\bar{H}_2}{\bar{H}_1}$, $\frac{k_2}{k_1}$ and ψ_1. Their effects are presented in tabular form with all numerical calculations carried out upto $m = n = 15$.

Tables 9 and 10 show the effect of varying $\frac{\bar{H}_2}{\bar{H}_1}$ and $\frac{k_2}{k_1}$ with varying M on $\bar{W}$ respectively. It may be observed that the increase in each of the ratios $\frac{\bar{H}_2}{\bar{H}_1}$ and $\frac{k_2}{k_1}$ has adverse affect on the load carrying capacity.

From Tables 11 to 13, it may be observed that the time of approach increases when (i) the magnetic field is increased (ii) ψ_1 decreases (iii) $\bar{h}$ decreases or (iv) $\frac{\bar{H}_2}{\bar{H}_1}$ decreases.

All tables confirm previous results [5] that the effect of an applied magnetic field greatly modifies the squeezing action.

TABLE 9

Values of dimensionless load capacity $\bar{W}$ for different values of $\frac{\bar{H}_2}{\bar{H}_1}$ and M. $\psi_1 = 0.01$, $d = 4$, $m_1 = m_2 = 0.6$, $\bar{h} = 0.5$, $\frac{k_2}{k_1} = 20$, $\frac{H}{A} = 0.02$ and $\frac{h_o}{A} = 0.001$.

M \ $\frac{\bar{H}_2}{\bar{H}_1}$	0.00	0.25	0.33	1.00	3.00	4.00
10	0.0456	0.0235	0.0211	0.0139	0.0099	0.0093
20	0.0657	0.0466	0.0435	0.0325	0.0254	0.0243
30	0.0898	0.0742	0.0711	0.0587	0.0495	0.0480
40	0.1214	0.1078	0.1049	0.0922	0.0819	0.0800

TABLE 10

Values of dimensionless load capacity $\bar{W}$ for different values of $\frac{k_2}{k_1}$ and M. $\psi_1 = 0.01$, $d = 4$, $m_1 = m_2 = 0.6$, $\bar{h} = 0.5$, $\frac{\bar{H}_2}{\bar{H}_1} = 4$, $\frac{H}{A} = 0.02$ and $\frac{h_o}{A} = 0.001$.

M \ $\frac{k_2}{k_1}$	0.0	1.0	5.0	10.0	20.0
10	0.1125	0.0456	0.0174	0.0122	0.0093
20	0.2193	0.0657	0.0323	0.0270	0.0243
30	0.3376	0.0898	0.0555	0.0505	0.0480
40	0.4816	0.1214	0.0871	0.0824	0.0800

TABLE 11

Values of ΔT for different values of $\bar{h}$ and $\frac{\bar{H}_2}{\bar{H}_1}$. $\psi_1 = 0.01$,

$d = 4$, $m_1 = m_2 = 0.6$, $M = 10$, and $\frac{k_2}{k_1} = 20$, $\frac{H}{A} = 0.02$ and $\frac{h_o}{A} = 0.001$.

$\frac{\bar{H}_2}{\bar{H}_1}$ \ $\bar{h}$	0.3	0.4	0.5	0.6	0.7	0.8
0.00	0.2327	0.1909	0.1527	0.1176	0.0851	0.0549
0.25	0.1246	0.1045	0.0852	0.0668	0.0491	0.0321
0.33	0.1124	0.0945	0.0772	0.0607	0.0447	0.0293
1.00	0.0753	0.0637	0.0524	0.0414	0.0307	0.0202
3.00	0.0543	0.0461	0.0381	0.0302	0.0224	0.0148
4.00	0.0509	0.0433	0.0358	0.0284	0.0211	0.0140

TABLE 12

Values of ΔT for different values of $\frac{\bar{H}_2}{\bar{H}_1}$ and M. $\psi_1 = 0.01$, d= 4, $m_1 = m_2 = 0.6$, $\frac{k_2}{k_1} = 20$, $\bar{h} = 0.5$, $\frac{H}{A} = 0.02$ and $\frac{h_o}{A} = 0.001$.

M \ $\frac{\bar{H}_2}{\bar{H}_1}$	0.00	0.25	0.33	1.00	3.00	4.00
10	0.1527	0.0852	0.0772	0.0524	0.0381	0.0358
20	0.2448	0.1771	0.1658	0.1252	0.0989	0.0946
30	0.3437	0.2860	0.2745	0.2280	0.1934	0.1874
40	0.4695	0.4186	0.4076	0.3595	0.3200	0.3129

TABLE 13

Values of ΔT for different values of $\frac{\bar{H}_2}{\bar{H}_1}$ and ψ_1. $d = 4$,

$m_1 = m_2 = 0.6$, $\frac{k_2}{k_1} = 20$, $\bar{h} = 0.5$, $M = 10$, $\frac{H}{A} = 0.02$ and $\frac{h_o}{A} = 0.001$.

ψ_1 \ $\frac{\bar{H}_2}{\bar{H}_1}$	0.00	0.25	0.33	1.00	3.00	4.00
0.0	0.4300	0.4300	0.4300	0.4300	0.4300	0.4300
0.001	0.3577	0.2508	0.2356	0.1809	0.1395	0.1316
0.01	0.1527	0.0852	0.0772	0.0524	0.0381	0.0358
0.1	0.0370	0.0312	0.0300	0.0251	0.0215	0.0208
1.0	0.0195	0.0191	0.0190	0.0185	0.0180	0.0179

3.2 HYDROMAGNETIC LUBRICATION OF AN INCLINED POROUS SLIDER BEARING

Snyder [46] and Fucks and Uhlenbusch [47] analysed the inclined slider bearing with a transverse magnetic field. They considered only the open circuit conditions. Moreover, their analyses involved unusual normalization of parameters which made physical interpretation a little difficult. Hughes [48] considered the same configuration for open circuit and short circuit conditions. He found that significant load increases could be effected by supplying external power and, for large Hartmann numbers, open circuit conditions could give rise to greatly increased load capacities. Agrawal [49] extended the above analysis by including the inertia effects. However, all the above investigators considered both the slider and the bearing to be impermeable.

Prakash and Vij [37] analysed the hydrodynamic lubricating characteristics of an inclined slider bearing when the slider was impermeable and the stator had a porous facing backed by a solid wall. They showed that the effect of porosity was to decrease the load capacity and friction but to increase the coefficient of friction.

It was shown by Sinha and Gupta [5] that hydromagnetic effects could be used to increase the bearing characteristics considerably without altering the size of the bearing.

In this section we study the effects of a transverse magnetic field on an inclined porous slider bearing with an electrically conducting lubricant.

3.2.1 Mathematical formulation

We consider a fluid film of thickness $h = h(x)$ within an inclined slider bearing, infinite in the z-direction, whose upper surface is non-porous and moves parallel to itself with a uniform velocity U. The lower surface has a porous facing of thickness H, backed by a solid wall. A uniform magnetic field B_0 is applied in the y-direction as in Fig. 8. Following the assumptions of porous metal hydromagnetic lubrication of section 1.2, the governing applicable equation as deduced from equation (39) of chapter 1 is

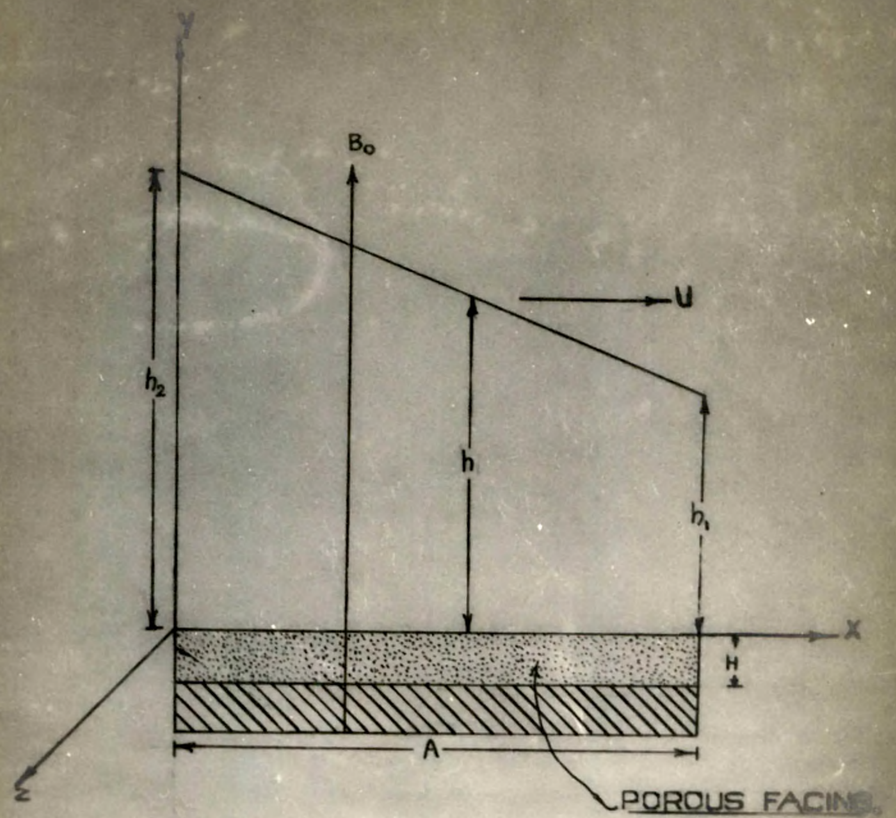

FIG. 8. POROUS INCLINED SLIDER WITH A TRANSVERSE MAGNETIC FIELD.

$$\frac{d}{dx}\left[\left(\frac{dp}{dx} + \sigma E_z B_0\right)\left\{\frac{kH}{c^2} + \frac{h_1^3}{M^3}\left(\frac{Mh}{h_1} - 2\tanh\frac{Mh}{2h_1}\right)\right\}\right]$$

$$= \frac{\mu U h_1}{M}\frac{d}{dx}\left(\tanh\frac{Mh}{2h_1}\right), \qquad (62)$$

where

$$c = \left(1 + \frac{k}{m^*}\frac{M^2}{h_1^2}\right)^{1/2}, \quad M = B_0 h_1 \sqrt{\sigma/\mu}$$

and

$$h = h_2 - (h_2 - h_1)x.$$

Introducing the dimensionless quantities

$$\left.\begin{aligned} &\bar{x} = \frac{x}{A}, \quad a = \frac{h_2}{h_1}, \quad \bar{h} = \frac{h}{h_1} = a - (a-1)\bar{x}, \\ &\bar{p} = \frac{h_1^2 p}{\mu U A} \quad \text{and} \quad \bar{E}_z = E_z \frac{h_1}{U}\sqrt{\sigma/\mu} \end{aligned}\right\} \qquad (63)$$

into equation (62) we have

$$\frac{d}{d\bar{x}}\left[\left(\frac{d\bar{p}}{d\bar{x}}+M\bar{E}_z\right)\left\{\frac{M^2}{c^2}\frac{kH}{h_1^3}+\left(\bar{h}-\frac{2}{M}\tanh\frac{M\bar{h}}{2}\right)\right\}\right]$$

$$=\frac{d}{d\bar{x}}\left(M\tanh\frac{M\bar{h}}{2}\right). \qquad (64)$$

Integrating equation (64) once with respect to $\bar{x}$ we have

$$\left(\frac{d\bar{p}}{d\bar{x}}+M\bar{E}_z\right)\left[\frac{2}{M}\tanh\frac{M\bar{h}}{2}-\bar{h}-\frac{M^2}{c^2}\frac{kH}{h_1^3}\right]$$

$$=M^2\left(Q_3-\frac{1}{M}\tanh\frac{M\bar{h}}{2}\right), \qquad (65)$$

where Q_3 is constant of integration.

In general, equation (65) cannot be integrated analytically, so we obtain its asymptotic solutions for large and small values of M.

3.2.2 Solutions for small Hartmann numbers

When M is small, equation (65) may be written in rearranged form as

$$\frac{d\bar{p}}{d\bar{h}} = -\frac{6}{a-1}\;\frac{\bar{h}+Q_4}{\bar{h}^3+\alpha^3} + \frac{M\,\bar{E}_z}{a-1} \tag{66}$$

where Q_4 is the constant used in place of Q_3 in the present case of small M and

$$\alpha^3 = 12\,\psi = \frac{12kH}{h_1^3}\,.$$

Solving equation (66) under the boundary conditions

$$\bar{p}\,(\bar{h}=a) = \bar{p}\,(\bar{h}=1) = 0, \tag{67}$$

we obtain the dimensionless pressure distribution as

$$\bar{p} = -\frac{1}{a-1}\left[\frac{1}{\alpha}\left\{L_1-L+2\sqrt{3}\,(T-T_1)\right\}\right.$$

$$\left.+\frac{Q_4}{\alpha^2}\left\{L-L_1+2\sqrt{3}(T-T_1)\right\} - M\bar{E}_z(\bar{h}-a)\right], \tag{68}$$

where

$$Q_4 = \alpha\,\frac{\alpha M\bar{E}_z(a-1)+L_1-L_2+2\sqrt{3}\,(T_2-T_1)}{L_1-L_2+2\sqrt{3}\,(T_1-T_2)} \tag{69}$$

and

$$L = \ln \left[\frac{(\bar{h}+\alpha)^2}{\bar{h}^2-\alpha\bar{h}+\alpha^2} \right], \quad T = \tan^{-1} \left(\frac{2\bar{h} - \alpha}{\alpha\sqrt{3}} \right)$$

and L_1, L_2 and T_1, T_2 are the values of L and T when $\bar{h} = a$ and $\bar{h} = 1$ respectively.

The dimensionless load capacity is

$$\bar{W} = \frac{h_1^2 W}{\mu U A^2 B} = \frac{1}{(a-1)^2} \left[2 \ln \left(\frac{a^3 + \alpha^3}{1 + \alpha^3} \right) \right.$$

$$\left. - \frac{Q_4}{\alpha} \left\{ L_1 - L_2 + 2\sqrt{3}\,(T_2 - T_1) \right\} + \bar{M}\bar{E}_z \frac{(1-a^2)}{2} \right] \quad (70)$$

The dimensionless frictional drag exerted by the moving slider is

$$\bar{F} = \frac{h_1 F}{\mu U A B} = \frac{1}{a - 1} \left[\ln \left(\frac{a^3 + \alpha^3}{1 + \alpha^3} \right) \right.$$

$$\left. - \frac{Q_4}{2\alpha} \left\{ L_1 - L_2 + 2\sqrt{3}\,(T_2 - T_1) \right\} \right] + \frac{\ln a}{a - 1} \quad (71)$$

The centre of pressure is given by

$$\frac{\bar{\bar{x}}}{A} = \frac{1}{2(a-1)^3\bar{\bar{W}}}\Big[6(1-a) + 2(Q_4 - 2a)\ln\left(\frac{1+\alpha^3}{a^3+\alpha^3}\right)$$

$$+ \frac{a^2 - 2a\,Q_4}{\alpha}\left\{L_1 - L_2 + 2\sqrt{3}\,(T_2 - T_1)\right\}$$

$$+ \frac{(a^2Q_4 - \alpha^3)}{\alpha^2}\left\{L_2 - L_1 + 2\sqrt{3}\,(T_2 - T_1)\right\} - M\bar{E}_z\,\frac{(1-a)^3}{3}\Big] \qquad (72)$$

Total current I per unit length is given by

$$I = \iint_{\Gamma} J_z\,dxdy = \iint_{\Gamma} \sigma\,(E_z + uB_0)\,dxdy \qquad (73)$$

where Γ is the area of the cross section of the flow in the xy plane.

The dimensionless current is

$$\bar{I} = \frac{I}{AU\sqrt{\sigma\mu}} = \frac{1}{12\left\{L_1 - L_2 + 2\sqrt{3}\,(T_1 - T_2)\right\}}$$

$$\cdot \Big[\bar{\bar{E}}_z \Big\{ \left[6(a+1) + M^2\alpha^3\right]\left[L_1 - L_2 + 2\sqrt{3}(T_1 - T_2)\right]$$

$$- 6(a-1)\ M^2\alpha^2 \Big\} - 6M\alpha \left\{L_1 - L_2 + 2\sqrt{3}\,(T_2 - T_1)\right\} \Big]. \qquad (74)$$

In the open circuit case, I = 0 so that equation (74) gives

$$\bar{\bar{E}}_z = \frac{6\ M\alpha\ \left[L_1 - L_2 + 2\sqrt{3}\,(T_2 - T_1)\right]}{\left[6(a+1) + M^2\alpha^3\right]\left[L_1 - L_2 + 2\sqrt{3}\,(T_1 - T_2)\right] - 6(a-1)\ M^2\alpha^2} \qquad (75)$$

In the short circuit case, $\bar{\bar{E}}_z = 0$, so that equation (74) gives

$$\bar{I} = -\frac{M\alpha}{2}\ \frac{L_1 - L_2 + 2\sqrt{3}\,(T_2 - T_1)}{L_1 - L_2 + 2\sqrt{3}\,(T_1 - T_2)}\ .$$

3.2.3 Solutions for large Hartmann numbers

When M is large, equation (65) may be written in rearranged form as

$$\frac{d\bar{p}}{d\bar{h}} = - \frac{1}{a-1} \left[M^2 \frac{Q_5 M - 1}{\alpha^* - M\bar{h}} - M\bar{E}_z \right], \tag{76}$$

where

$$\alpha^* = 2 - \frac{M^3}{c^2} \psi \tag{77}$$

and Q_5 is the constant used in place of Q in the case of large M.

Solving equation (76) under the boundary conditions (67) we have the dimensionless pressure distribution as

$$\bar{p} = M\bar{E}_z \left[\frac{\ln\left(\frac{M\bar{h} - \alpha^*}{Ma - \alpha^*} \right)}{\ln\left(\frac{M - \alpha^*}{Ma - \alpha^*} \right)} + \frac{\bar{h} - a}{a - 1} \right]. \tag{78}$$

The dimensionless load capacity is given by

$$\bar{W} = - M\bar{E}_z \left[\frac{1}{2} + \frac{M - \alpha^*}{M(a-1)} + \frac{1}{\ln\left(\frac{M - \alpha^*}{Ma - \alpha^*} \right)} \right]. \qquad (79)$$

The dimensionless frictional drag is

$$\bar{F} = M + \bar{E}_z \qquad (80)$$

The centre of pressure is given by

$$\frac{\bar{\bar{X}}}{A} = \frac{\bar{E}_z}{\bar{W}(a-1)^2} \left[\frac{1-a}{4} \cdot \frac{M - 3aM + 2\alpha^*}{\ln\left(\frac{Ma - \alpha^*}{M - \alpha^*} \right)} - \frac{(Ma - \alpha^*)^2}{2M} + \frac{M}{6}(a-1)^2 \right]. \qquad (81)$$

The dimensionless current is

$$\bar{I} = \frac{I}{AU\sqrt{\sigma\mu}} = \bar{E}_z \left[\frac{a+1}{2} + \frac{a-1}{\ln\left(\frac{M-\alpha^*}{Ma-\alpha^*}\right)} + \frac{2-\alpha^*}{M} \right] + 1 \qquad (82)$$

In the open circuit case, I = 0 so that equation (82) gives

$$\bar{E}_z = -2 \frac{\ln\left(\frac{M-\alpha^*}{Ma-\alpha^*}\right)}{\left(a+1+\frac{4-2\alpha^*}{M}\right)\ln\left(\frac{M-\alpha^*}{Ma-\alpha^*}\right)+2(a-1)} . \quad (83)$$

In the short circuit case, $\bar{E}_z = 0$ so that equation (82) gives $\bar{I} = 1$.

3.2.4 Results and discussion

By setting $M = 0$ in 3.2.2, one can obtain the results of hydrodynamic lubrication of an inclined porous slider [37].

By setting $\psi = 0$ in 3.2.3, we have the results for a non-porous hydromagnetic inclined slider bearing [48].

In other words, the section 3.2 generalizes both the analyses [37, 48].

Since small values of M do not significantly increase the load capacity, we compute the bearing characteristics for large M. We consider the open circuit case the results for which are displayed in figures 9, 10 and Table 14.

Fig. 9 is a plot of $\bar{W}$ vs ψ for various values of M. It is clear from this figure that significant increases in load capacity can be made by increasing M.

Fig. 10 shows that the dimensiomless friction increases with M.

It is seen from Table 14 that the centre of pressure shifts to the middle of the bearing when ψ or M increases. The shift due to ψ is not more pronounced than the shift due to the intensity of the applied magnetic field.

All the Tables show that the hydromagnetic inclined porous slider behaves like an impermeable one for large values of the Hartmann number. However, the self-lubricating nature of a porous bearing is maintained without significantly affecting the other bearing characteristics.

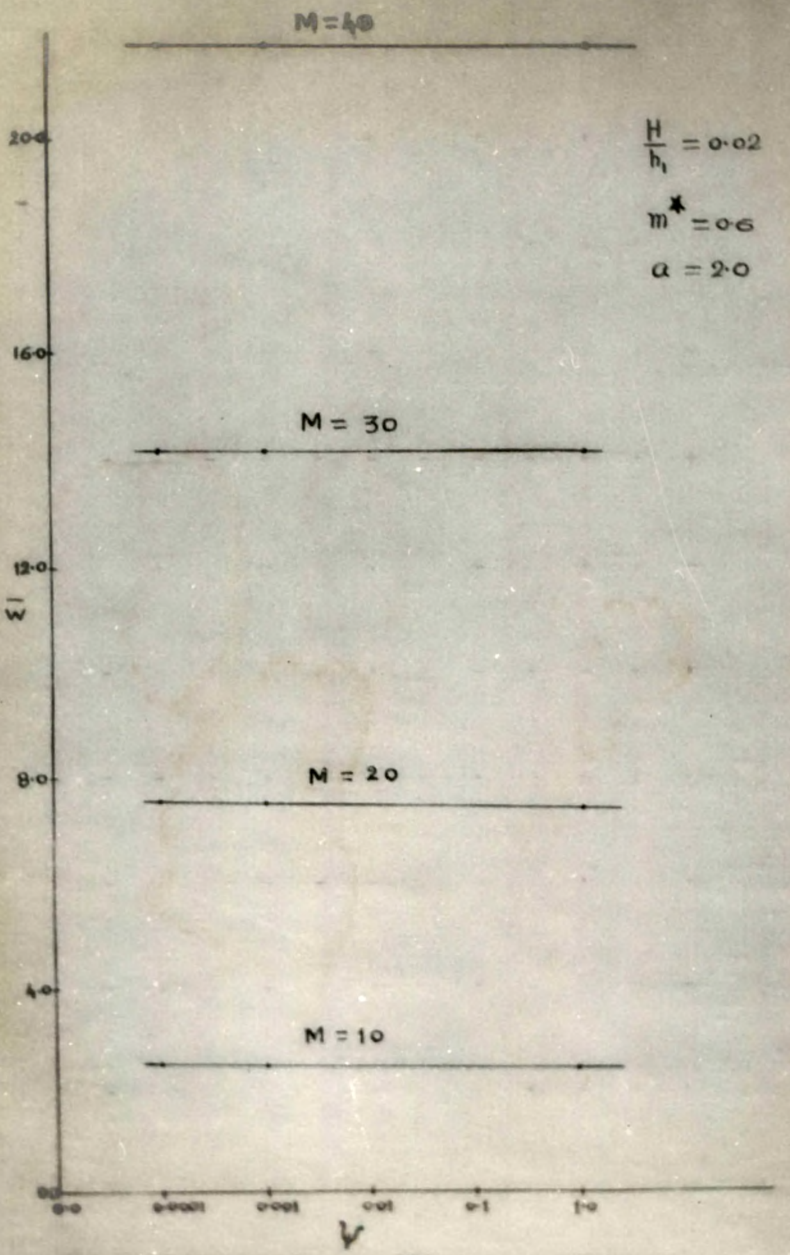

FIG. 9. PLOT OF $\bar{W}$ VS. ψ FOR VARIOUS VALUES OF M.

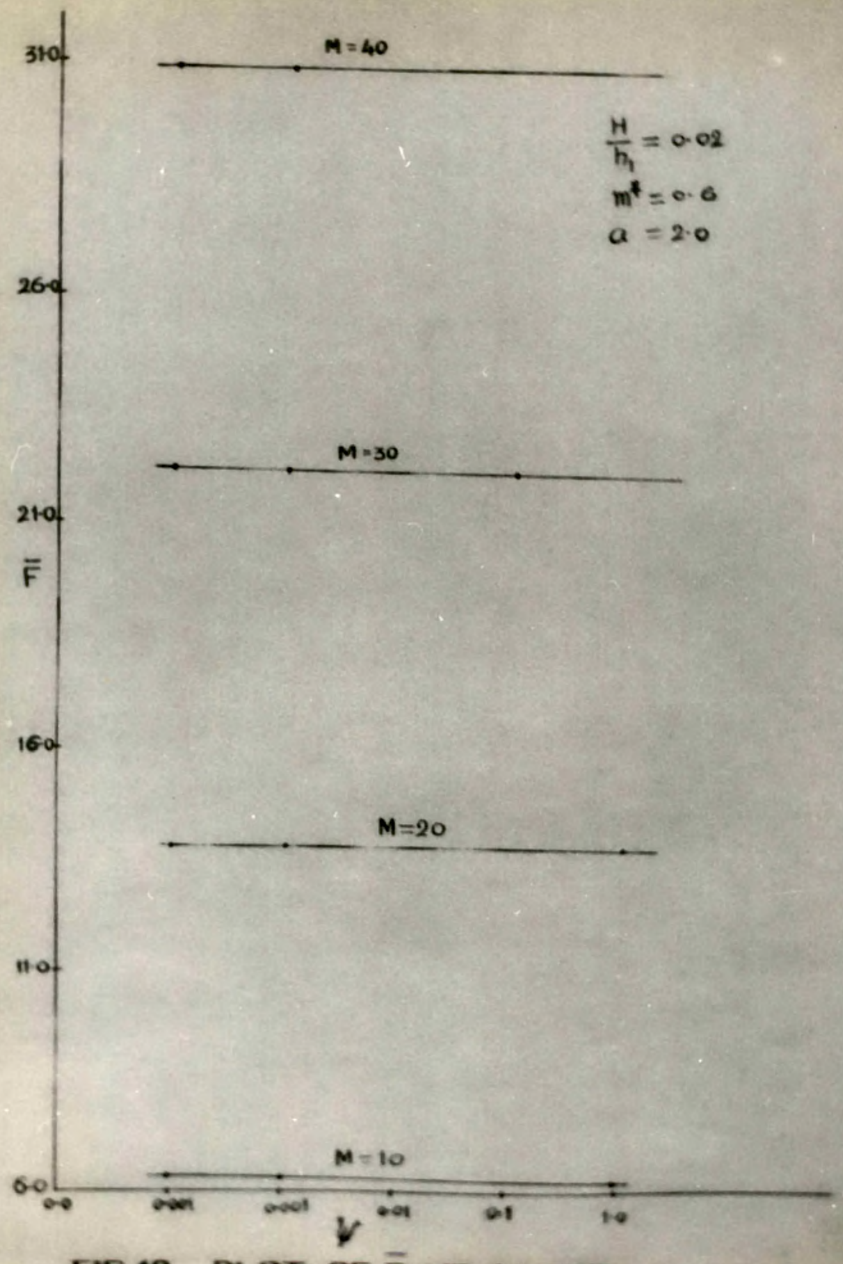

FIG.10. PLOT OF $\bar{F}$ VS. ψ FOR VARIOUS VALUES OF M.

TABLE 14

Values of dimensionless centre of pressure for various values of ψ and M.

$\frac{H}{h_1} = 0.02$, $m^* = 0.6$ and $a = 2$.

M \ ψ	0.0000	0.0001	0.0010	0.0100	0.1000	1.0000
10	0.5267	0.5266	0.5265	0.5264	0.5264	0.5264
20	0.5246	0.5245	0.5244	0.5244	0.5244	0.5244
30	0.5240	0.5238	0.5238	0.5238	0.5238	0.5238
40	0.5237	0.5235	0.5235	0.5235	0.5235	0.5235